Open access • Journal Article • DOI:10.1109/TPWRS.2009.2034748

Model Predictive Control-Based Real-Time Power System Protection Schemes

— Source link

Licheng Jin, Ratnesh Kumar, Nicola Elia

Institutions: Iowa State University

Published on: 01 May 2010 - IEEE Transactions on Power Systems (IEEE)

Topics: Voltage regulation, Voltage optimisation, Voltage droop, Voltage source and Model predictive control

Model Predictive Control based Real Time Power System Protection Schemes

Licheng Jin, *Member, IEEE,* and Ratnesh Kumar, *Fellow, IEEE,* and Nicola Elia, *Member, IEEE*

***Abstract*—The objective of power system controls is to keep the electrical flow as well as voltage magnitudes within acceptable limits in spite of the load and network topology changes. The control of voltage level is accomplished by controlling the production, absorption as well as flow of reactive power at various locations in the system. This paper presents an approach to determine a real time system protection scheme for maintaining voltage stability following the occurrence of a contingency by means of reactive power control. This approach is based on the Model Predictive Control (MPC) theory. According to an economic criterion and control effectiveness, a control switching strategy consisting of a sequence of amounts of the shunt capacitors to switch is identified for voltage restoration. The effect of the capacitive control on voltage recovery is measured via trajectory sensitivity. This approach is applied to the WECC system to enhance the performance of voltage and to the 39 bus New England system for preventing voltage collapse.**

***Index Terms*—Model predictive control, trajectory sensitivity, voltage stabilization, switching control, power system**

I. Introduction

As a result of deregulation as well as increasing demands, power systems operate close to their capacity. Although power systems are designed with proper planning and with proper stability margin, the instability can still occur under certain severe disturbances. It is imperative that schemes for power system protection be in place to mitigate their catastrophic effects such as large scale shutdowns and collapses. The objective of SPSs is to detect a potential instability or a safety/security degradation of a power system and carry out the necessary control actions to mitigate their effects (such as a partial shutdown or a total collapse).

The traditional SPS is determined off-line and is rule based [1], [2], [3]. A rule based system protection scheme relies on voltage, or their rate of change levels, or line flow limits. For example, if the measured voltage is lower than a specific value, or the line flow exceeds the line rating limit, a predefined SPS is triggered (such as adjustment of generator outputs or load shedding). The limitation of the rule based SPSs lies in the use of limited local information. In contrast, a real time SPS computes and carries out control actions based on global state information in response to an impending contingency detected by an online dynamic security assessment program. Recent advances in monitoring, communication, and computing technologies have greatly facilitated the implementation of real-time SPSs [4].

A real time system protection scheme for voltage stabilization is studied in this work. The control of voltage level is accomplished by controlling the production, absorption, and flow of reactive power at various locations in the system. With regard to a power system, sources and/or sinks of reactive power, such as shunt capacitors, shunt reactors, synchronous condensers, and static var compensators (SVCs) are used to control voltage level. In literature, many algorithms [5], [6], [7] have been developed to determine the amounts and locations of shunt reactive power compensation devices needed for maintaining a satisfactory voltage profile, while minimizing their cost.

Most these work however are based on *static analysis*, which means that the voltage performance criteria could be met only if the system reaches a post-contingency stable operating point. However, if the disturbances are sever, the power system may lose stability. Under this situation, the control strategy to restore the stable equilibrium point requires a *dynamic analysis*.

Model predictive control has been applied in power system voltage control based on dynamic analysis. [8] presents a method of coordination of load shedding, capacitor switching and tap changers using model preventive control. The prediction of states is based on the numerical simulation of nonlinear differential algebraic equations (DAEs) together with Euler state prediction. A tree search method is adopted to solve the optimization. [9] proposes a coordination of generator voltage setting points, load shedding and ULTCs using a heuristic search and the predictive control. The prediction of states is based on the linearization of nonlinear DAEs. [10] presents an optimal coordinated voltage control using model predictive control. The controls used include: shunt capacitors, load shedding, tap changers and generator voltage setting points. The prediction of voltage trajectory is based on the Euler state prediction. The optimization problem is solved by a pseudo gradient evolutionary programming (PGEP) technique. In [11] and [12], authors present a method to compute a voltage emergency control strategy based on model predictive control. The prediction of the output trajectories is based on trajectory sensitivity. However, in these two papers, the authors employ a simplified model predictive control, which computes the control actions only at the initial time and implements it over the entire control horizon. A voltage stabilization control strategy

The work was supported in part by the National Science Foundation under Grants NSF-ECCS-0424048, NSF-ECCS-0601570, NSF-ECCS-0801763, and NSF-CCF-0811541.

L. Jin is with the Department of Electrical and Computer Engineering of Iowa State University, Ames, IA 50011, USA and also with California ISO, Folsom, CA, 95630 USA (email:ljin@caiso.com)

R. Kumar is with the the Department of Electrical and Computer Engineering of Iowa State University, Ames, IA 50011, USA (email:rkumar@iastate.edu)

N. Elia is with the the Department of Electrical and Computer Engineering of Iowa State University, Ames, IA 50011, USA (email:nelia@iastate.edu)

is also proposed in [13] based on load shedding, where the objective function is to minimize the amount of load shedding required to restore the voltages. It shows load shedding is an effective voltage control under emergency condition. [14] presents a MPC based voltage control design. The controls are reference voltage of automatic voltage regulators and load shedding.

In this paper, we propose computation of the optimal strategies based on *model predictive control* (MPC). We utilize shunt capacitors for control purposes as they are effective means of voltage stabilization. The problem then becomes one of determining capacitor switching sequence and amounts given their locations and limits which are determined in a prior planning stage (see for example [15]), together with the requirements on the magnitudes of voltages. In this work, the trajectory deviation and the cost of controls are simultaneously minimized. Here, trajectory deviation refers to the deviation of voltage trajectory from the nominal value. This is a multi-objective optimization and a positively weighted convex sum is chosen as the objective function. Trajectory sensitivities are used to estimate the effect of controls on the voltage behavior in a linear manner. Due to the use of model predictive approach, the influence of each optimization is limited to one step and the control gets recalculated and refined at each step, the overall control strategy turns out to be sound and robust. The features of our work, compared to the prior works dealing with dynamic analysis, is summarized as follows:

- Trajectory sensitivity is used to compute a 1st-order (linear) approximation of the effect of control without having to linearize the system model. Further at each control step, the trajectory sensitivity is updated (based on a prediction of system trajectory starting from an estimate of the current state under the control applied in the past steps). This way of computing the effect of control provides a better approximation as compared to [8], [9], [10], where either system linearization or numerical simulation of DAEs was used.
- Optimization minimizes costs of control as well as voltage-deviations. In contrast [13], only considers the amount of controls to restore the voltage.
- Optimization at each control step is a quadratic programming problem, and hence can be efficiently solved. In contrast [10] uses a pseudo gradient evolutionary programming. [8], [9] use a tree search method.
- In contrast to [11] and [12], where the control action is calculated only at the initial time, and remains the same over the entire control horizon, a sequence of control inputs is determined and only the first of them is applied in our case.
- [14] presented a voltage control strategy based on reference voltage of automatic voltage regulators and load shedding. [13] applied MPC for load-shedding computation. This paper presents an MPC-based shunt capacitor control for voltage stabilization, a commonly used control mechanism in North America power grid.

II. Background

A. Model predictive control

Model Predictive Control (MPC) refers to a class of algorithms that compute a sequence of manipulated variable adjustments in order to optimize the future behavior of a plant. An introduction to the basic concepts of MPC and a formulation can be found in [16]. The principle of MPC is graphically depicted in Fig. 1. Here x represents the state variable that needs to be controlled to a specific range. The available control is represented by variable u.

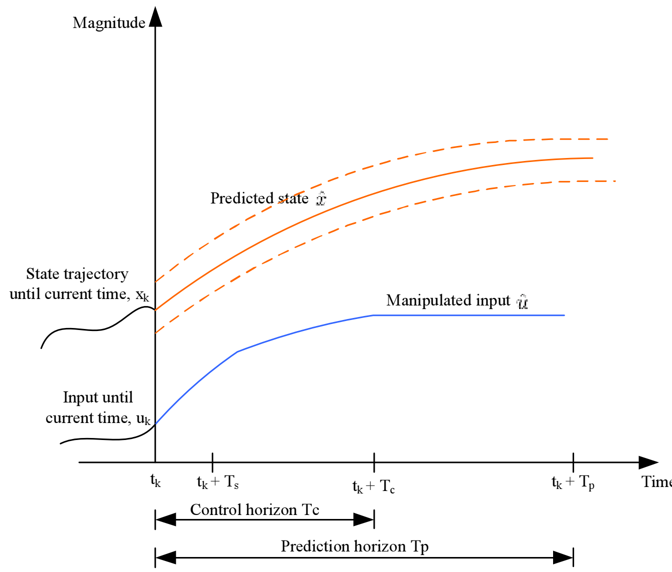

Fig. 1. Principle of MPC

At a current time t_k, the MPC solves an optimization problem over a finite prediction horizon $[t_k, t_k + T_p]$ with respect to a predetermined objective function such that the predicted state variable $\hat{x}(t_k + T_p)$ can optimally stay close to a reference trajectory. The control is computed over a control horizon $[t_k, t_k + T_c]$, which is smaller than the prediction horizon ($T_c \leq T_p$). If there were no disturbances, no model-plant mismatch and the prediction horizon is infinite, one could apply the control strategy found at current time t_k for all times $t \geq t_k$. However, due to the disturbances, model-plant mismatch and finite prediction horizon, the true system behavior is different from the predicted behavior. In order to incorporate the feedback information about the true system state, the computed optimal control is implemented only until the next measurement instant ($t_k + T_s$), at which point the entire computation is repeated.

In a MPC, the optimization problem to be solved at time t_k can be formulated as follows:

$$\min_{\hat{u}} \int_{t_k}^{t_k+T_p} F(\hat{x}(\tau), \hat{u}(\tau)) d\tau \tag{1}$$

subject to

$$\dot{\hat{x}}(\tau) = f(\hat{x}(\tau), \hat{u}(\tau)), \quad \hat{x}(t_k) = x(t_k) \tag{2}$$

$$u_{min} \leq \hat{u}(\tau) \leq u_{max}, \quad \forall \tau \in [t_k, t_k + T_c] \tag{3}$$

$$\hat{u}(\tau) = \hat{u}(t_k + T_c), \quad \forall \tau \in [t_k + T_c, t_k + T_p] \tag{4}$$

$$x_{min}(\tau) \leq \hat{x}(\tau) \leq x_{max}(\tau), \quad \forall \tau \in [t_k, t_k + T_p] \tag{5}$$

Here, T_c and T_p are the control and prediction horizon with $T_c \leq T_p$. $\hat{x}$ denotes the estimated state and $\hat{u}$ represents "estimated" control (The true state may be different and the true control matches the estimated control only during the first sampling period).

Equation (1) represents the cost function of the MPC optimization. Equation (2) represents the dynamic system model with initial state $x(t_k)$. Equations (3) and (4) represent the constraints on the control input during the prediction horizon. Equation (5) indicates the state operation requirement during the prediction horizon.

B. Trajectory sensitivity

Consider a differential algebraic equation (DAE) of a system,

$$\begin{aligned} \dot{x} &= f(x, y, u), \quad x(0) = x_0 && (6) \\ 0 &= g(x, y, u) && (7) \end{aligned}$$

where x is a vector of state variables, y is a vector of algebraic variables, and u is a vector of control variables. Trajectory sensitivity considers the influence of small variations in the control u (and any other variable of interest) on the solution of the state equations (6) and (7). Let u_0 be a nominal value of u, and assume that the nominal system in (8) and (9) has a unique solution $x(t, x_0, u_0)$ over $[t_0, t_1]$.

$$\begin{aligned} \dot{x} &= f(x, y, u_0), \quad x(0) = x_0 && (8) \\ 0 &= g(x, y, u_0) && (9) \end{aligned}$$

Then the system in Equations (6) and (7) has a unique solution $x(t, x_0, u)$ over $[t_0, t_1]$ that is related to $x(t, x_0, u_0)$ as:

$$\begin{aligned} x(t, x_0, u) &= x(t, x_0, u_0) + x_u(t)(u - u_0) + \text{H.O.T} && (10) \\ y(t, x_0, u) &= y(t, x_0, u_0) + y_u(t)(u - u_0) + \text{H.O.T} && (11) \end{aligned}$$

Here $x_u(t) = \frac{\partial x(t, x_0, u)}{\partial u}$ is called the trajectory sensitivities of state variables with respect to variable u and $y_u(t) = \frac{\partial y(t, x_0, u)}{\partial u}$ is the trajectory sensitivities of algebraic variables with respect to variable u.

The evolution of trajectory sensitivities can be obtained by differentiating Equations (6) and (7) with respect to the control variables u and is expressed as:

$$\dot{x}_u(t) = f_x(t)x_u(t) + f_y(t)y_u(t) + f_u(t) \tag{12}$$

$$0 = g_x(t)x_u(t) + g_y(t)y_u(t) + g_u(t) \tag{13}$$

Detailed information about trajectory sensitivity theory can be found in [17]. The trajectory sensitivity can be solved numerically. [18] provides a methodology for the computation of trajectory sensitivity. When time domain simulation of a power system is based on trapezoidal numerical integration, the calculation of trajectory sensitivity requires solving a set of linear equations, thus costing a little time. In our work, we extended the Power System Analysis Tool [19] (a MATLAB based tool) to do trajectory sensitivity calculation and the MPC optimization.

Fig. 2 illustrates the application of trajectory sensitivity in evaluating the effect of controls on system behavior. The trajectory x_k of the nominal system represents the behavior under the control u_k. When the control is increased by Δu_1^k at time t_k, the change in predicted system behavior based on sensitivity analysis at time t_l, can be approximated as $\Delta x_1^{kl} = x_{u_1^k}^l \Delta u_1^k$. Here $x_{u_1^k}^l$ is the trajectory sensitivity of the state variable at time t_l with respect to the control at time t_k. Similarly if we increase the control by Δu_n^k at time $t_k + (n-1)T_s$, the change in the state variable at time t_l is represented by $\Delta x_n^{kl} = x_{u_n^k}^l \Delta u_n^k$. Here, $x_{u_n^k}^l$ is the trajectory sensitivity of the state variable at time t_l with respect to the control at time $t_k + (n-1)T_s$.

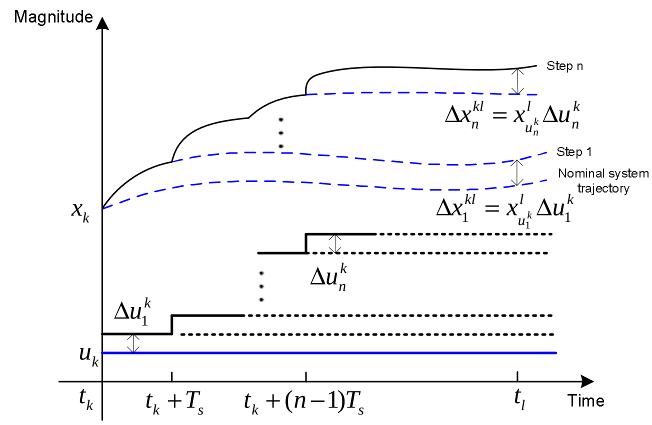

Fig. 2. Application of trajectory sensitivity in system behavior prediction

III. Problem Formulation and Solution

The purpose of this work is to find an effective and economic control strategy for controlling the shunt capacitors so as to eliminate voltage instability following any pre-identified contingency. For analyzing voltage performance following disturbances, we model generator and automatic voltage regulator (AVR) as well as aggregated exponential dynamic load models [20], [21]. The overall power system is represented by a set of differential algebraic equations (DAE) as in Equations (6) and (7). Here x is a vector of states including state variables in generator dynamic models, AVR models and dynamic load models such as, rotor angles and angular speeds of generators, outputs of AVRs, and active power recovery and reactive power recovery of dynamic load models. y is a vector of algebraic variables such as bus voltage magnitudes and phase angles. The vector u indicates the output of shunt capacitors. The computation is iterative over a finite control horizon, where in each step a quadratic programming problem is solved to compute the amounts of shunt capacitors to be added in that step. The quadratic programming formulation is valid when the capacitor control is continuous as in SVC. Even in the case where capacitor control is discrete, we can still proceed by assuming continuous control so as to compute an optimal control by solving a quadratic programming relaxation. Then for implementation, the nearest discrete control value can be applied. Any error will get propagated to a following control step, and where it will get corrected. The control is piecewise constant, changing only at the sampling times. Let T_p be the prediction horizon, T_c be the control horizon, T_s be the control sampling interval, and $N = \frac{T_c}{T_s}$ be the total number of control steps. The procedure to determine the control strategy at time t_k based on MPC is as follows:

Step 1: At time t_k (i.e. the $(k+1)^{th}$ sampling instant), an estimate of the current state $x(t_k)$ is obtained. The nominal power system evolves according to Equations (6) and (7). Here, $u = \{B_m^0 + \sum_{i=0}^{k-1} \Delta B_{m1}^i\}_{m=1}^{m=M}$ is the control variable (i.e. amounts of shunt capacitors currently in use). B_m^0 is the amounts of shunt capacitors that exist at time 0. $\sum_{i=0}^{k-1} \Delta B_{m1}^i$ is the amounts of shunt capacitors that were added over time $[0, t_k - T_s]$. Time domain simulation is used to obtain the trajectory of the nominal system (6) and (7), starting from the state $x(t_k)$ at time t_k to the end of prediction horizon $t_k + T_p$. At the same time, the trajectory sensitivity of bus voltages with respect to the shunt capacitors to be added at instants $t_k + (n-1)T_s, n = 1 \ldots N-k$ is obtained and denoted as $V_{B_{mn}}^{kj}(t)$ (see below for the explanation of notation).

Step 2: At time t_k, solve the optimization problem over the prediction horizon $[t_k, t_k + T_p]$ and the control horizon $[t_k, t_k + T_c]$ as stated in (14)-(18). The objective function is composed of two parts. The first term is the trajectory deviation, the second term is the cost of controls. The combination of the deviation of voltages from nominal values and the control cost needs to be minimized. The number of candidate control locations and their upper limits are determined through a prior planning step (see for example [15]). The total number of control variables in the optimization is the number of candidate control locations times the number of control steps. The optimization is solved in Matlab, and it does converge to a global minimum.

Minimize (with respect to ΔB_{mn}^k)

$$\int_{t_k}^{t_k+T_p} (\widehat{V}^k(t) - V_{ref})' R (\widehat{V}^k(t) - V_{ref}) dt + \sum_{mn} W_{mn} \Delta B_{mn}^k \tag{14}$$

Subject to

$$\Delta B_m^{min} \le \Delta B_{mn}^k \le \Delta B_m^{max} \tag{15}$$

$$B_m^{min} \le B_m^0 + \sum_{i=0}^{k-1} \Delta B_{m1}^i + \sum_{n=1}^{N} \Delta B_{mn}^k \le B_m^{max} \tag{16}$$

$$V_{min}^{kj}(t) \le V^{kj}(t) + \sum_{m=1}^{M} \sum_{n=1}^{\min(N,l)} V_{B_{mn}}^{kj}(t) \Delta B_{mn}^k \le V_{max}^{kj}(t) \tag{17}$$

$$\Delta B_{mn}^k \ge 0 \tag{18}$$

- R is the weight matrix. $\widehat{V}^k(t)$ is the predicted voltage vector at the control sampling time t_k that contains all the bus voltages in the system at time t. ΔB^k is the control matrix calculated at time t_k.
- W_{mn} is the weighted cost of control m to be added at time $t_k + (n-1)T_s$.
- M is the total number of control variables, i.e. the number of shunt capacitor locations.
- N is the total number of control steps.
- ΔB_{mn}^k is the entry ΔB^k, which is the amount of control m to be added at time $t_k + (n-1)T_s$.
- $\Delta B_m^{min} \in \Re$ is the minimum amount of control m to be added at any step.
- $\Delta B_m^{max} \in \Re$ is the maximum amount of control m to be added at any step.
- ΔB_{m1}^i is the amount of control m implemented at the control sampling point $t_i, i = 0, \ldots k-1$.
- $B_m^{min} \in \Re$ is the minimum amount of control m that must be used, typically 0.
- $B_m^{max} \in \Re$ is the maximum available amount of control m.
- $V^{kj}(t) \in \Re$ is the voltage of bus j at time $t (t_k \le t \le t_k + T_p)$, of the nominal system of time t_k.
- $V_{min}^{kj}(t)$ is the minimum voltage at bus j desired at time $t_k \le t \le t_k + T_p$.
- $V_{max}^{kj}(t)$ is the maximum voltage at bus j desired at time $t_k \le t \le t_k + T_p$.
- $V_{B_{mn}}^{kj}(t)$ is the trajectory sensitivity of voltage at bus j at time $t_k \le t \le t_k + T_p$ with respect to control m added at time $t_k + (n-1)T_s$.

Step 3: At time t_k, a solution of the optimization problem (14)-(18) computes a sequence of controls ΔB_{mn}^k. Add only the first control ΔB_{m1}^k at time t_k and observe or estimate the system state $x(t_{k+1})$ at time $t_{k+1} = t_k + T_s$

Step 4: Increase k by $k+1$ and repeat steps (1)-(3) until the $k = N-1$.

A. Implementation

The functional structure of a real time SPS is shown in Figure 3. Line flow, bus voltage information, switch status as well as phase measurement unit (PMU) measurements are sent to a control center through communication channels of a SCADA system. These measurements plus a network model are used by the state estimator (SE) for filtering out the noise and making best use of the measured data. The results from the state estimator are used for power flow analysis. A power flow solution is then used by an on-line dynamic security assessment program to initialize the state variables of the dynamic models. Further, it uses system models and disturbance information to perform the contingency analysis to evaluate the security margin of the power system. If a contingency is identified where the system will become unstable, the MPC based SPS computation will get triggered at the time an identified critical contingency occurs. The steps of the MPC computation in the k^{th} iteration include:

- Estimate static variables such as voltage magnitudes and angles at time t_k as well as the dynamic variables $x(t_k)$ such as generator angles, velocities and real and reactive load recovery.
- Run time-domain simulation to compute the system trajectory given the current state. This step also requires the knowledge of a complete system model (including both dynamic and static components).
- Obtain trajectory sensitivities of voltage with respect to the control variables as a by-product of the time-domain simulation performed in the previous step. This

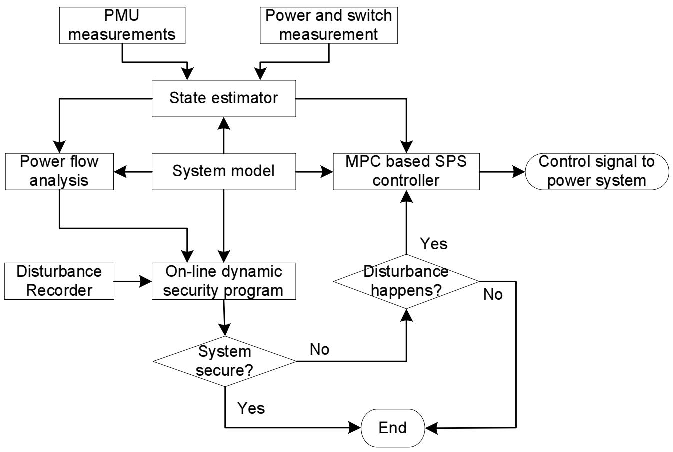

Fig. 3. Structure of a real time SPS

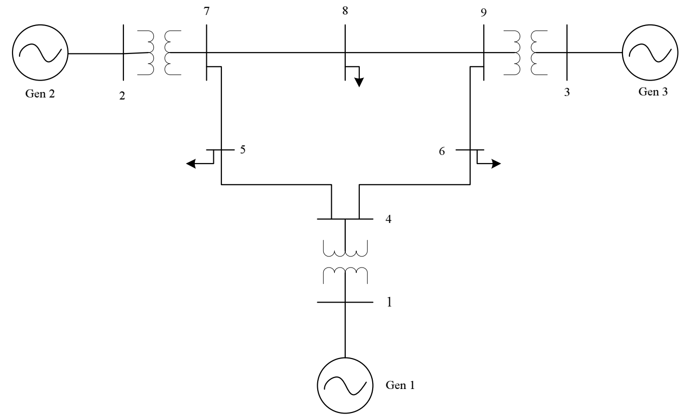

Fig. 4. WECC 3-generator 9-bus test system

is required for the prediction of system response given a certain control strategy.

- Solve the quadratic programming optimization problem and implement the first step of the control.
- Repeat the above steps at each sampling point until the end of control horizon.

Remark: While we suggested an on-line computation of MPC based SPS above, it is also possible to do this computation off-line based on the predicted (rather estimated) values of the states and trajectory sensitivities.

IV. Application to WECC and to New England Systems

The proposed method has been applied to the WECC 9-bus system as well as to the New England 39-bus system. The exponential recovery load model is used in both cases. The parameters of the load model are as following:

$$T_p = T_q = 30, \alpha_s = 0, \alpha_t = 1, \beta_s = 0, \beta_t = 4.5.$$

The parameters in MPC optimization are determined based on the following considerations. Any voltage instability following a contingency must be stabilized in a certain time duration (typically the time in which voltage will decrease by 15%). This is the prediction horizon T_p. The control should be exercised on a time horizon T_c, which is shorter than the prediction horizon, typically the time in which voltage will decrease by 10% (if no control is applied). A discrete-time control must be applied within this duration T_c at a sample-rate high enough to adequately react to the changing voltage trajectory, as well as to allow accurate enough predictions of the voltage trajectory based on the linearization of the trajectory-sensitivity. This dictates the sampling duration T_s. The number of sampling point N is then determined as the ratio of T_c and the sampling duration T_s.

A. WECC 3-generator 9-bus test system

1) System description: Figure 4 is a representation of the WECC 3-generator 9-bus system. A fourth-order model is used for modeling each of the three generators. The state variables include the rotor angle δ, the rotor speed ω, the q-axis transient voltage e'_q, and the d-axis transient voltage e'_d. Automatic Voltage Regulator (AVR) defines the primary voltage regulation for generator 1. The continuously acting regulator and exciter model [22] is employed in this study. It is represented by a four-dimensional state equation. The loads at buses 5, 6 and 8 are taken to be exponential recovery dynamic load and each load is described by a two-dimensional state equation. Therefore, the total dimension number of the state space is 22. At buses 5, 7 and 8, there exist shunt capacitors for voltage regulation. These are the control variables. Under normal conditions, all of the shunt capacitors are disconnected.

2) Fault scenario: We consider a three-phase fault at bus 5 at $t = 1.0$ second, which is cleared at $t = 1.2$ seconds by the tripping of the line between bus 4 and bus 5. Based on the time domain simulation, the voltages at buses 5, 7 and 8 are shown in Fig. 5 and are not satisfactory. At $t = 1.0$ second, the voltages begin to drop dramatically due to the three phase to ground fault. At $t = 1.2$ seconds, the voltages start to recover since the fault gets cleared. However, the voltages begin to oscillate. 15 seconds later, voltages begin to decline gradually. The dynamic load models result in slightly recovery load consumption, which deteriorate the voltage condition. These three voltages fall out of the lower limit 0.95 p.u 1 minutes later. According to the system's operational criteria, the load bus voltages must be above 0.95 p.u. Therefore, some control actions are required to satisfy the criterion that the voltages outlined above remain above 0.95 p.u.

3) Simulation result: In this example, we have chosen prediction horizon T_p to be 40 seconds (the time in which voltage drops by nearly 15% at bus 5). T_c has been chosen to be 35 seconds. We found that a sampling duration of T_s = 7 seconds works well for this example, and so we have the number of control steps: $N = \frac{T_c}{T_s} = \frac{35}{7} = 5$. Model predictive control approach determines the amounts of shunt capacitors to be added at each sampling instant so as to recover the local voltages. Although the capacitors have a positive effect on low voltage problems, the maximum capacitor to be added at any step ΔB_m^{max} was set to be 0.1 p.u. This is because if large amounts of capacitors are added at one time, an over-voltage may occur, which has a bad effect on the electrical devices of

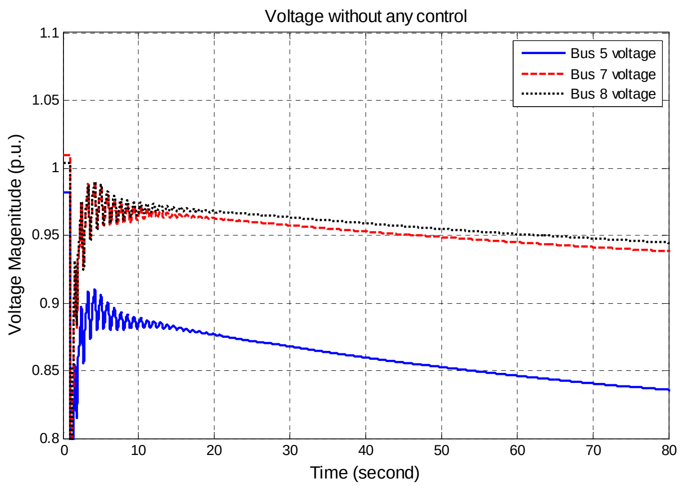

Fig. 5. Voltage behavior of WECC system without MPC control

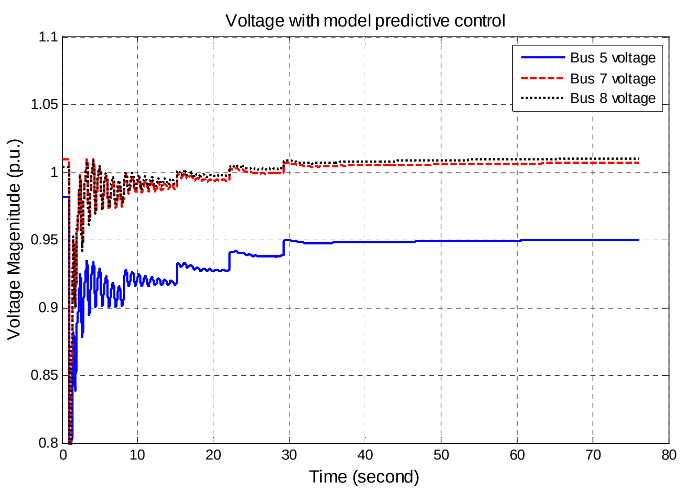

Fig. 6. Voltage behavior of WECC system with MPC control

the power system. During the optimization, we set the lower bound of all bus voltages to be 0.95 p.u. and upper bound of load bus voltages to be 1.05 p.u. For other buses, such as a generator bus, we set the maximum voltage magnitude to be 1.08 p.u., a bit higher than a load bus. These settings are practical. Fig. 6 shows the bus voltages after MPC based control was implemented starting at time $t = 1.2$ seconds. From the figure, we can see that all the bus voltages were restored to above 0.95 p.u and the oscillations of the voltages disappeared within 35 seconds.

The control strategy is shown in Table I. Suppose the control action starts right after the fault is cleared. The first control action happens at $t = 1.2$ seconds. 0.1 p.u. capacitors at buses 5, 7 and 8 were added. The sample duration is 7 seconds as explained in the last paragraph. Therefore, the second control action happens at $t = 8.2$ seconds. The third, fourth and fifth control steps happen at 15.2 seconds, 22.2 seconds and 29.2 seconds respectively.

B. New England 10-generator 39-bus test system

1) System description: Fig.7 represents the New England 10-generator 39-bus system. All the generator models are

TABLE I
THE RESULTING CONTROL STRATEGY FOR WECC SYSTEM

Time(second)	1.2	8.2	15.2	22.2	29.2
Capacitor at bus 5 (p.u.)	0.1	0.1	0.1	0.1	0.0981
Capacitor at bus 7 (p.u.)	0.1	0	0	0	0
Capacitor at bus 8 (p.u.)	0.1	0	0	0	0

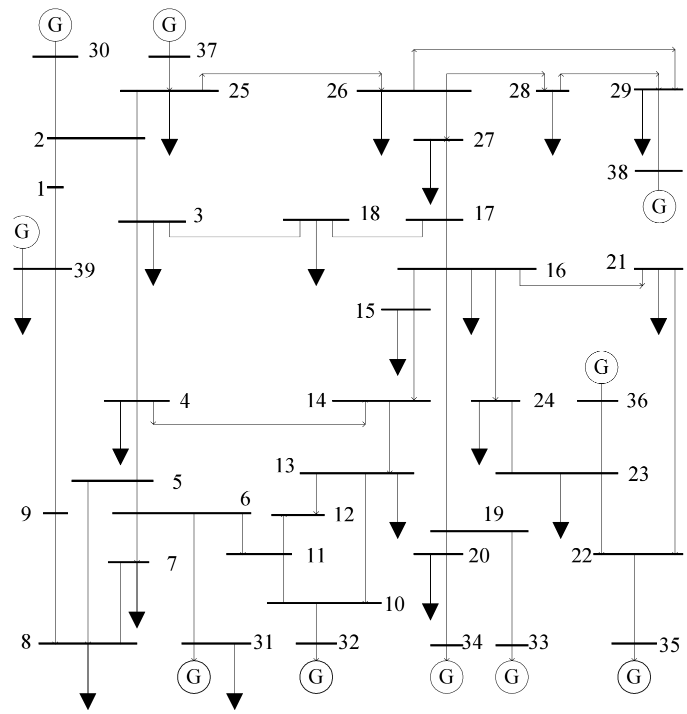

Fig. 7. New England 10-generator 35-bus test system

taken to have a fourth order state-space consisting of the rotor angle δ, the rotor speed ω, and the q-axis transient voltage e'_q and the d-axis transient voltage. The exception is the generator at bus 39 for which only a third-order model is used that does not include the d-axis transient voltage as part of the state-space. In addition, all the generators except generators at buses 34, 37 have automatic voltage regulators (AVRs), which are represented by fourth-order models. The load models used in the time domain simulation are exponential recovery dynamic loads. The total dimension of the state space is 131. The control variables include the shunt capacitors that are located at buses 16, 20, 22, 23 and 34. Under normal conditions, none of the shunt capacitors is in use.

2) Fault scenario: The contingency considered here is a three-phase to ground fault at bus 21 at $t = 1.0$ second, which is cleared at $t = 1.1$ seconds and by the tripping of the transmission line between bus 21 and bus 22. The voltage drops dramatically when the fault occurs as seen in Fig. 8. After the fault is cleared at 1.1 seconds, the voltages recover around 0.95 p.u, although some oscillations proceed. About 30 seconds later, the oscillations disappear, but all the voltages start to decline very slowly. Then around 2 minutes later, the voltages collapse. One reason for the voltage recovery is the presence of generator automatic voltage regulators. When the system voltage drops following the fault, AVRs start to increase the generator excitation voltages so as to support the

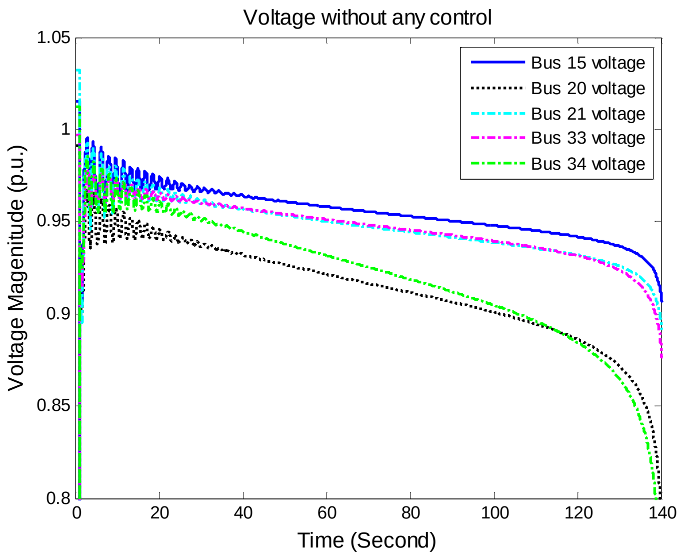

Fig. 8. Voltage behavior of New England system without MPC control

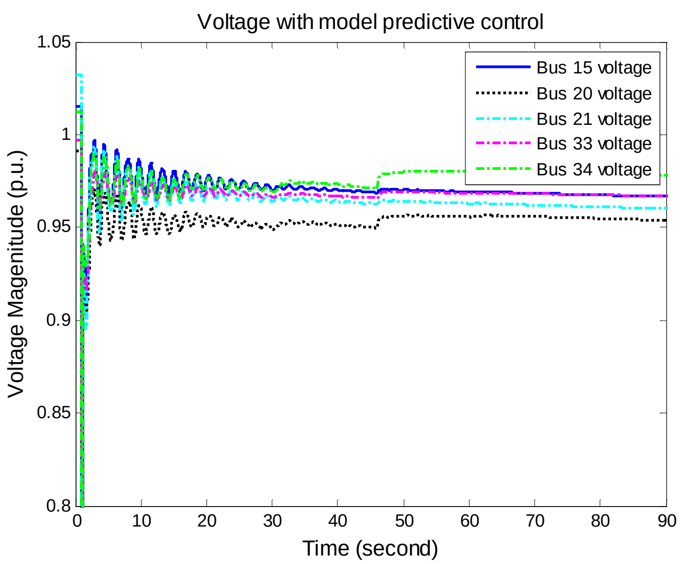

Fig. 9. Voltage behavior of New England system with MPC control

TABLE II
THE RESULTING CONTROL STRATEGY FOR NEW ENGLAND SYSTEM

Time(second)	1.1	16.1	31.1	46.1	61.1
Capacitor at bus 16 (p.u.)	0	0	0	0	0
Capacitor at bus 20 (p.u.)	0	0	0	0	0
Capacitor at bus 22 (p.u.)	0	0	0	0	0
Capacitor at bus 23 (p.u.)	0	0	0	0	0
Capacitor at bus 34(p.u.)	0.1	0.0889	0.0896	0.1	0.0259

system voltage. However, AVRs have their upper limits. At the same time, the exponential recovery of the loads during the voltage disturbance worsen the operation of the system. The system can not fully recover from the contingency considering these two factors, which lead to the voltage collapse.

3) Simulation result: In this example, we have chosen prediction horizon T_p to be 80 seconds (the time in which voltage drops by nearly 10% at bus 20). T_c has been chosen to be 75 seconds. We found that a sample duration of $T_s = 15$ seconds works well for this example, and so we have the number of control steps: $N = \frac{T_c}{T_s} = \frac{75}{15} = 5$. The control strategy is determined by our model predictive control approach. The system response with MPC in place is shown in Fig. 9. The corresponding control strategy is shown in Table II. The first control step happens right after the fault is cleared, i.e. 1.1 seconds. Since the sampling interval is 15 seconds, the second control happens at 16.1 seconds. The third, fourth and fifth control steps happen at 31.1 seconds, 46.1 seconds and 61.1 seconds respectively.

V. COMPARISON WITH TRADITIONAL LOCAL FEEDBACK CONTROL

Shunt capacitors such as SVCs can also be used as in the setting of traditional local feedback control. The mathematical formulation of the local feedback control can be expressed as follows.

$$\dot{B} = \frac{1}{T_r}(K_r(V_{ref} - V) - B) \qquad (19)$$

where K_r is regulation gain, V_{ref} is reference voltage, T_r is regulation time constant. V is the voltage magnitude of the regulated bus. B is the control amount. For the traditional local feedback control, shunt capacitor adjusts its output based on the voltage of the controlled bus.

Compared with traditional local feedback control, the proposed control scheme is more effective since it involves global state feedback and global control. The state of the entire power system is taken into consideration in deciding the global control. The WECC system discussed in Section IV can be used to illustrate this point. Suppose there are two shunt capacitors in the WECC system which are located at buses 5 and 6. Both SVCs have a capacity of 0.5 p.u.. The system data and fault scenario are the same as in section IV. Under no fault, the voltage magnitudes of buses 5 and 6 are 0.9819 p.u. and 0.9981 p.u. respectively. For local feedback control we set these values as the reference voltages at buses 5 and 6 respectively. Therefore, when there is no fault, the outputs of the shunt capacitors are zero. Suppose the regulation gain K_r is 100 and the regulation time constant T_r is 0.5 second. After the fault happens, Figure 10 depicts the dynamic behavior of voltage magnitudes at buses 5 and 6. Although the voltage at bus 6 is acceptable, the voltage at bus 5 is unsatisfactory (< 0.95 p.u.). Figure 11 shows the outputs of the SVCs at buses 5 and 6. Under no fault, the output of the SVCs are zero. When fault happens, the voltage at bus 6 drops dramatically, and the output of SVC at bus 6 increases immediately based on the local feedback control to boost the voltage at bus 6. However, after around 5 seconds, the output of the SVC returns to zero since the voltage at bus 6 is greater than the reference value. The output of the SVC at bus 5 reaches its maximum value. Yet the voltage magnitude at bus 5 remains below the desired value. From this simulation, we can see that local feedback control based SVC only maintains the voltage of the regulated bus. It doesn't offer control for any unsatisfactory voltage behavior at other buses.

For the case discussed above, we also use the proposed MPC-based method to design control. The parameters for the

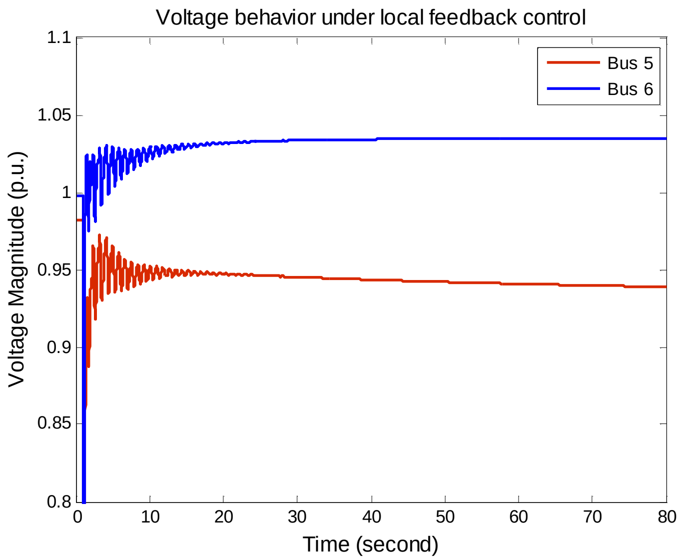

Fig. 10. Voltage behavior of WECC system under local feedback control

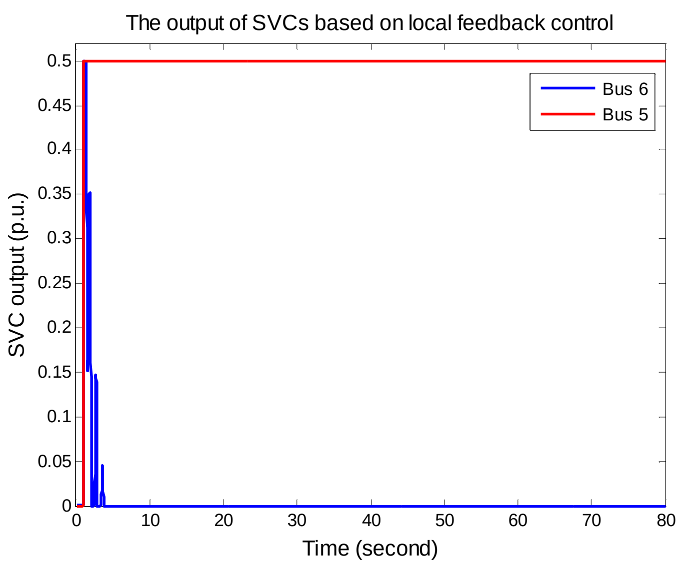

Fig. 11. The output of SVC based on local feedback control

MPC control are the same as in Section IV. The resulting control strategy is described as follows. At time 1.2 seconds, 0.5 p.u. of SVC control is added at bus 5 and 0.123 p.u. of SVC control is added at bus 6. At times 8.2 seconds and 15.2 seconds no control is added. At time 22.2 seconds, 0.0053 p.u. control is added at bus 6. At time 29.2 seconds, another 0.005 p.u. of SVC control is added at bus 6. The voltage behaviors at buses 5 and 6 under the MPC based control design are shown in Figure 12. From this figure, we can see that voltage behavior at bus 5 under the proposed method is better than that under local feedback control. From this simulation, we can see that the main difference between the proposed method and the local feedback control is that the proposed method makes use of all the available controls in the system to improve voltage performance of all the buses. In contrast, the local feedback control based method makes use of only the local controls. (In the above example, control at bus 6 is not being used to

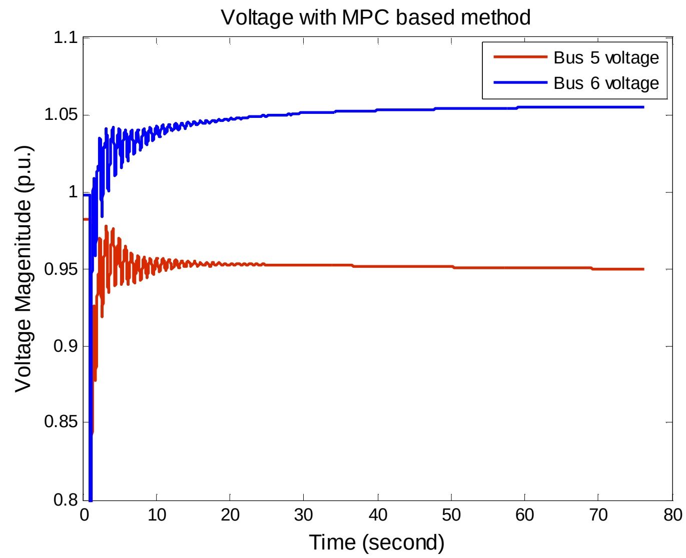

Fig. 12. Voltage behavior of WECC system with MPC

compensate for performance at bus 5.)

VI. Robustness Study

The impact of data uncertainty on the performance of model based control methodologies is an important issue. In this section, the designed control is tested for robustness over different operating conditions using time domain simulation. Our study is based on the 9-bus 3-generator WECC example of Section IV for which the control scheme is as shown in Table I. Since load plays an important role in voltage stability problem, our robustness study mainly focuses on the effect of load change, and consists of two parts. The first part is to study the effect of base case load variation on the robustness of the designed control. The second part studies the robustness of the designed control when random disturbances happen on the dynamic state variables of the load model.

A. Base case load increase

This part studies the robustness of the designed control when the total base case load increases. Figure 13 shows the voltage behavior of 1 % load increase. From this figure, we can see that the control scheme is still valid under the small load variation. Figure 14 indicates the voltage behavior of the same system with 3 % load increase. Although the voltages are stable, the voltage magnitude on bus 5 is lower than 0.95 p.u.. This study shows, under small load variation, the designed control is still valid

B. Random disturbance on an individual load

Besides the base case load change, we also study the effect of random disturbance on the dynamic state variable of an individual load. Assume the random disturbance is represented by a statistical variable with normal distribution whose mean is zero and variance is 1. In our study, a Matlab function *Normrnd* is used to generate the disturbance. The disturbance is imposed to the active power recovery P_r of the load at bus

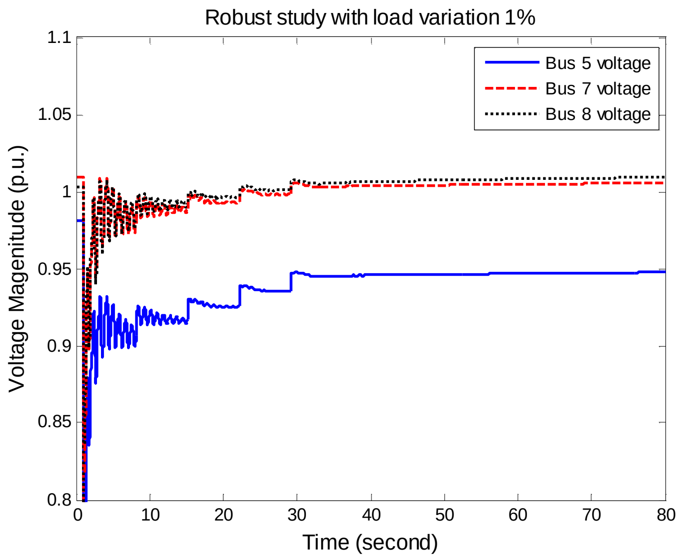

Fig. 13. Voltage behavior with the designed control under 1% load increase

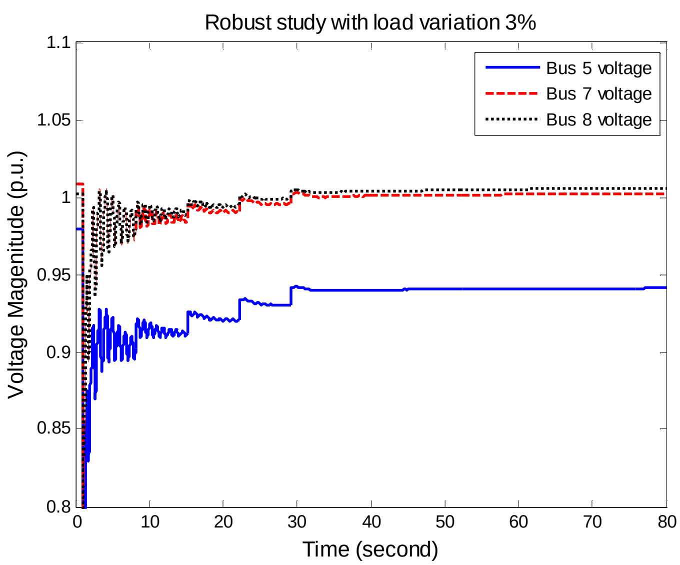

Fig. 14. Voltage behavior with the designed control under 3% load increase

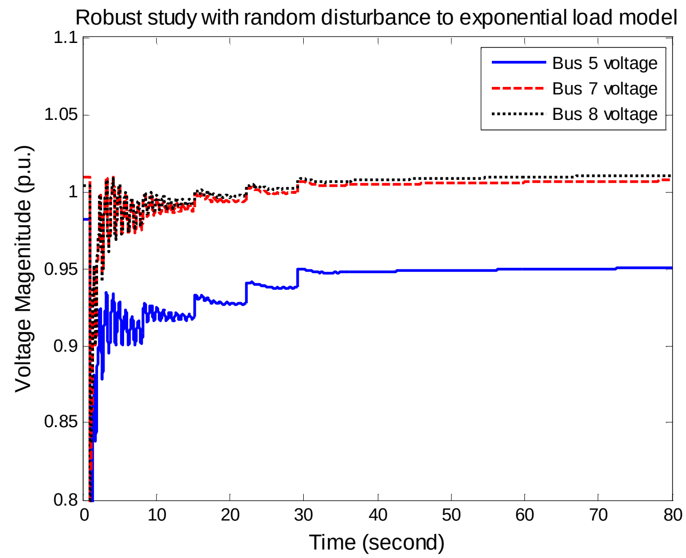

Fig. 15. Voltage behavior with the designed control with 0.7258 increase for dynamic state variable 17

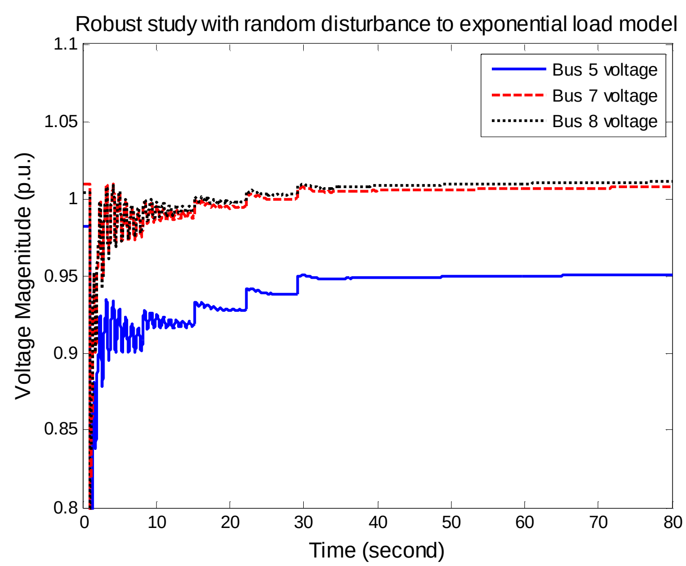

Fig. 16. Voltage behavior with the designed control with 0.5883 decrease for dynamic state variable 17

6 at control sampling point 3. The first disturbance generated by the the Matlab program is 0.7258 increase of the dynamic state variable of the exponential recovery load model at bus 6. The voltage behavior under such disturbance is shown in Figure 15. The second disturbance is 0.5883 decrease of the same dynamic state variable. Figure 16 indicates the dynamic voltage behavior under the disturbance. These two figures show that the designed control has a certain robustness against random load disturbances.

VII. Conclusion and Discussion

This paper introduces a model predictive control based system protection scheme for maintaining voltage stability under contingencies. The stabilizing control is achieved through the economic use of shunt capacitors. Trajectory sensitivity is used to establish the relationship between the control systems and the voltage recovery, which provides for a more accurate measurement of the influence of control. Further the feature of model predictive control, that at each control instant implements only the first step of the computed control sequence, corrects the errors brought by the approximation of system models. The WECC and New England systems are employed to illustrate the effectiveness of the control strategies.

In the numerical simulation, maximum value for control variables for each step is set as 0.1. This value is used only for illustration. In fact our formulation allows arbitrary values for the bounds, denoted B^{max}, ΔB^{max} in Equation (15) and Equation (16). By solving the quadratic programming problem of the formulation given by equations (14)-(18), an optimal solution is always obtained.

References

[1] S. Bernard, G. Trudel, and G. Scott, "A 735 kv shunt reactors automatic switching system for Hydro-Quebec network," *IEEE Transactions on Power Systems*, vol. 11, no. 4, pp. 2024–2030, 1996.

[2] G. Trudel, S. Bernard, and G. Scott, "Hydro-quebec's defence plan against extreme contingencies," *IEEE Transactions on Power Systems*, vol. 3, no. 14, pp. 958–965, 1999.

[3] B. Otomega and T. V. Cutsem, "Undervoltage load shedding using distributed controllers," *IEEE Transactions on Power Systems*, vol. 22, no. 4, pp. 1898–1907, 2007.

[4] K. Tomsovic, D. E. Bakken, V. Venkatasubramanian, and A. Bose, "Designing the next generation of real-time control, communication, and computations for large power systems," in *Proceeding of the IEEE*, May 2005, pp. 965–979.

[5] N. Yorino, E. E. El-Araby, H. Sasaki, and S. Harada, "A new formulation for FACTS allocation for security enhancement against voltage collapse," *IEEE Transactions on Power Systems*, vol. 18, no. 1, pp. 3–10, 2003.

[6] Y. L. Chen, "Weak bus-oriented optimal multi-objective VAr planning," *IEEE Transactions on Power Systems*, vol. 11, no. 4, pp. 1885–1890, 1996.

[7] S. Granville and M. C. A. Lima, "Application of decomposition techniques to VAr planning: methodological and computational aspects," *IEEE Transcations on Power Systems*, vol. 9, no. 4, pp. 1780–1787, 1994.

[8] M. Larsson, D. J. Hill, and G. Olsson, "Emergency voltage control using search and predictive control," *International Journal of Power and Energy Systems*, vol. 24, no. 2, pp. 121–130, 2002.

[9] M. Larsson and D. Karlsson, "Coordinated system protection scheme against voltage collapse using heuristic search and predictive control," *IEEE Transactions on Power Systems*, vol. 18, no. 3, pp. 1001–1006, 2003.

[10] J. Y. Wen and Q. H. Wu, "Optimal coordinated voltage control for power system voltage stability," *IEEE Transactions on Power Systems*, vol. 19, no. 2, pp. 1115–1122, 2004.

[11] M. Zima, P. Korba, and G. Andersson, "Power systems voltage emergency control approach using trajectory sensitivities," in *Proceedings of 2003 IEEE Conference on Control Applications*, Istanbul, Turkey, 2003, pp. 189–194.

[12] M. Zima and G. Andersson, "Stability assessment and emergency control method using trajectory sensitivies," in *Proceedings of 2003 IEEE Bologna Power Tech Conference*, Bologna, 2003, p. 7.

[13] I. A. Hiskens and B. Gong, "MPC-based load shedding for voltage stability enhancement," in *44th IEEE Conference on Decision and Control*, Seville,Spain, 2005, pp. 4463–4468.

[14] M. Zima and G. Andersson, "Model predictive control employing trajectory sensitivities for power systems applications," in *Proceedings of the 44-nd IEEE Conference on Decision and Control*, Seville,Spain, 2005, pp. 4452–4456.

[15] H. Liu, L. Jin, J. D. McCalley, R. Kumar, and V. Ajjarapu, "Planning minimum reactive compensation to mitigate voltage instability," in *Proceedings of 2006 IEEE Power Engineering Society General Meeting*, Montreal, Canada, 2006, pp. 4452–4456.

[16] J. Rawlings, "Tutorial overview of model predictive control," *IEEE Control Systems Magazine*, vol. 20, no. 3, pp. 38–52, 2000.

[17] H. K. Khalil, *Nonlinear System (Third Edition)*. New Jeasey: Prentice Hall, 2002.

[18] I. A. Hiskens and M. A. Pai, "Trajectory sensitivity analysis of hybrid systems," *IEEE Transactions on Circuits and Systems*, vol. 47, no. 2, pp. 204–220, 2000.

[19] F. Milano, "An open source power system analysis toolbox," *IEEE Transactions on Power Systems*, vol. 20, no. 3, pp. 1199–1206, 2005.

[20] D. Karlsson and D. Hill, "Modeling and identification of nonlinear dynamic loads in power systems," *IEEE Transactions on Power Systems*, vol. 9, no. 1, pp. 157–166, 1994.

[21] D. Hill, "Nonlinear dynamic load models with recovery for voltage stability studies," *IEEE Transactions on Power Systems*, vol. 8, no. 1, pp. 166–176, 1993.

[22] I. C. Report, "Computer representation of excitation systems," *IEEE Transactions on Power Apparatus and Systems*, vol. PAS-87, no. 6, pp. 1460–1464, 1968.

Licheng Jin received the bachelor's degree in 2000 and master's degree of science in 2003 from Zhejiang University, Hangzhou, China. She is currently working towards the Ph.D. from Department of Electrical and Computer Engineering, Iowa State University, Ames. She joined California ISO, Folsom, CA, as a Network Application Engineer in 2007.

Ratnesh Kumar received the B.Tech. degree in Electrical Engineering from the Indian Institute of Technology at Kanpur, India, in 1987, and the M.S. and the Ph.D. degree in Electrical and Computer Engineering from the University of Texas at Austin, in 1989 and 1991, respectively. From 1991-2002 he was on the faculty of University of Kentucky, and since 2002 he has been on the faculty of the Iowa State University. He has held visiting positions at Univ. of Maryland at College Park, NASA Ames, Applied Research Lab. at Penn. State, Argonne National Lab.—West, and United Technology Research Center. He is a Fellow of the IEEE.

Nicola Elia received the Laurea degree in electrical engineering from Politecnico di Torino, in 1987 and the Ph.D. degree in electrical engineering and computer science from the Massachusetts Institute of Technology in 1996. Presently he is an Associate Professor in the Department of Electrical and Computer Engineering at Iowa State University. His research interests include computational methods for controller design and hybrid systems.